Articles

Comparison of NH Exchange and Circular Dichroism as Techniques for Measuring the Parameters of the Helix−Coil Transition in Peptides†

Carol A. Rohl*,‡ and Robert L. Baldwin

Department of Biochemistry, Stanford University School of Medicine, Stanford, California 94305

Received March 21, 1997; Revised Manuscript Received May 12, 1997⊗

ABSTRACT: Circular dichroism and NH exchange are compared directly as techniques for measuring helix content in peptides and the parameters of the helix−coil transition. To cover a broad range of helix contents, alanine-based peptides with chain lengths varying from 12 to 22 residues are examined over the temperature range from 0.6 to 26.9 °C in 1 M sodium chloride, ^2H_2O. Helix−coil transition theory independently fits both circular dichroism and exchange data, but the helix contents measured by exchange are larger than those measured by circular dichroism. The two techniques are brought into agreement by removing the assumption that the intrinsic chemical exchange rate in the helix is the same as the exchange rate measured for short unstructured model peptides. This modification allows the circular dichroism and NH exchange data to be described by the same set of helix parameters and indicates that the intrinsic exchange rate in the presence of helical structure is reduced approximately 17% relative to the rates measured in unstructured models. To test the possibility that this effect is electrostatic in origin, the sensitivity of the exchange reaction to ionic strength is determined. A substantial dependence of exchange rate on ionic strength is found, but the form of the dependence is complex. In studies of the exchange rates of native proteins, the exchange-competent form of the protein is assumed to exchange with the same rate constant as a blocked dipeptide with the identical amino acid sequences. Our result suggests that this assumption will be seriously in error in some cases because of charge effects in the protein.

Circular dichroism, CD,[1] is the primary method used to quantitate helix formation in alanine-based peptides: ellipticity at 222 nm, θ_{222}, increases linearly with the extent of helix formation. The main limitation of circular dichroism is that it is sensitive only to the average properties of a partially helical peptide. Consequently, while the average helix content of a peptide can be measured, the distribution of helical and nonhelical residues within a peptide cannot be determined. NH exchange provides both site-specific and quantitative measurement of helix formation. Under conditions of base-catalyzed exchange, the degree of protection from exchange directly measures the extent of hydrogen bonding by the peptide NH [Rohl & Baldwin, 1994; see also Englander and Kallenbach (1984)]. Because exchange occurs from nonhelical residues, NH exchange is sensitive to the equilibrium constant for helix formation. Consequently NH exchange and CD are complementary in the measurement of helix content and in their sensitivity. CD is optimally sensitive around 50% mean helix content, where small changes in free energy yield large changes in ellipticity. As peptides approach complete helix formation, the sensitivity of θ_{222} to helix content decreases. NH exchange increases in sensitivity, however, with increasing helix content, and small amounts of nonhelical structure are easily detectable.

In this study, we directly compare NH exchange and circular dichroism as techniques for measuring the parameters of the helix−coil transition. A series of peptides with the sequence Ac-(AAKAA)$_n$GY-NH$_2$ and differing chain lengths are examined over the temperature range from 0.6 to 26.9 °C so that helix contents cover the regions of optimal sensitivities of both techniques. The modified Lifson−Roig model for the helix−coil transition (Lifson & Roig, 1961; Rohl et al., 1996) is used to compare the results obtained with the two techniques. Ellipticity at 222 nm can be linearly converted to mean helix content and fitted using helix−coil transition theory to obtain the helix parameters. Because peptides of varying chain lengths are studied, a unique set of helix parameters which predict the relative helix contents of different chain lengths can be determined. Interpretation of θ_{222} requires that the base line ellipticities of the complete helix and the random coil be known. The random coil base line has been measured directly, and the helical base line has been estimated by extrapolation using short peptide data (Luo & Baldwin, 1997).

Interpretation of NH exchange kinetics also requires that the base line exchange properties be known. In the simplest model for exchange, no exchange occurs from a helical, hydrogen-bonded NH. A nonhelical or non-hydrogen-bonded amide proton exchanges with the intrinsic rate constant, k_{int}. The value of k_{int} is generally determined using unstructured model compounds (Molday et al., 1972; Bai & Englander, 1993; Rohl & Baldwin, 1994). The rate at which

† This work was supported by a grant from the National Institutes of Health (GM 31475).

* To whom correspondence should be addressed.

‡ Current address: Department of Biochemistry, University of Washington, P.O. Box 357742, Seattle, WA 98195.

⊗ Abstract published in *Advance ACS Abstracts,* June 15, 1997.

[1] Abbreviations: CD, circular dichroism; FPLC, fast protein liquid chromatography; FAB, fast atom bombardment; NMR, nuclear magnetic resonance; FID, free induction decay.

S0006-2960(97)00667-3 CCC: $14.00

the NH of a partially helical residue exchanges is directly proportional to the fraction of time that the NH is hydrogen bonded. Total NH exchange kinetics, which are measured here, are also sensitive to the distribution of helical residues. If the helix−coil transition were a two-state reaction between completely helical and completely unfolded forms, the total NH exchange kinetics would follow a single exponential decay. Observed kinetic curves deviate significantly, however, from single-exponential behavior. At early time points, more exchange is observed than predicted by the single exponential, because the end residues are frayed and less helical than average. At long time points, the exchange curve is dominated by central residues which are more helical than the average, and consequently exchange more slowly than predicted by the single exponential. Fitting the modified Lifson−Roig model to the shape of the total NH exchange curves allows, consequently, a unique set of helix parameters to be determined by NH exchange, and the reliability of the fit is much improved by studying peptides with the same repeating sequence and varying chain lengths.

Direct comparison of the helix parameters measured by NH exchange and CD provides a sensitive test of the procedures used to interpret data from the two techniques. NH exchange and CD, although complementary in sensitivity, both measure the extent of helix formation, and consequently the same set of helix parameters should predict the observed mean helix content, which is measured both by CD and total NH exchange, and the hydrogen-bonding pattern in the peptide, which is monitored by NH exchange. Here we find that the modified Lifson−Roig model independently fits both NH exchange and ellipticity data, but larger helix propensities are obtained by NH exchange. The same set of helix parameters does predict both the mean helix content and the hydrogen bonding pattern for both the CD and the NH exchange data if the intrinsic rate of exchange in the helix is allowed to differ from the exchange rate constants observed for model compounds. On average, the intrinsic exchange rate in a partly helical peptide is approximately 17% slower than the rate measured in short unstructured peptides. Analysis of NH exchange behavior in alanine-based peptides has been used previously to investigate the mechanism of protection from acid- and base-catalyzed exchange (Rohl & Baldwin, 1994). We show here that NH exchange data from alanine-based peptides, when normalized to be consistent with CD data, can be used to test further the model for exchange.

EXPERIMENTAL PROCEDURES

Peptide Synthesis and Purification. Peptides were synthesized by stepwise solid phase procedures using fluorenylmethyloxycarbonyl (Fmoc) amino acids. Fmoc amino acids with free acids were coupled using 2-(1*H*-benzotriazol-1-yl)-1,1,3,3-tetramethyluronium tetrafluoroborate (TBTU) in the presence of *N*-methylmorpholine. Pentafluorophenyl esters of Fmoc amino acids were coupled using 1-hydroxybenzotriazole (HOBt). N-termini were acetylated using pyridine and acetic anhydride. C-terminal carboxamide blocking groups were provided by the use of Rink resin (Advanced ChemTech, Louisville, KY). Peptides were purified by reverse-phase FPLC on C18 resin in gradients of acetonitrile containing 0.1% trifluoroacetic acid. Peptide purity was greater than 95%, as shown by reverse phase FPLC. Molecular weights were confirmed by FAB mass spectrometry.

Circular Dichroism Measurements. Peptide stock solutions for CD measurements were made 0.5−1.0 mM in water and filtered before use. Concentrations of stock solutions were determined by measurement of tyrosine absorbance at 275 nm in 6.5 M guanidine hydrochloride, 20 mM potassium phosphate, pH 6.5 using $\epsilon_{275\text{nm}} = 1450\ \text{M}^{-1}\ \text{cm}^{-1}$ (Brandts & Kaplan, 1973). CD measurements were made on an Aviv 60DS spectropolarimeter equipped with a Hewlett-Packard 89100A temperature control unit using quartz cuvettes with 1.0 mm pathlengths. Ellipticity was calibrated with (+)-10-camphorsulfonic acid and is reported as mean molar residue ellipticity, $[\theta]$ (deg cm^2 dmol^{-1}). The temperature inside the cuvette was measured using a Bat-12 digital thermometer (Sensortek, Inc) equipped with a Physitech temperature probe (model NJ07013). CD spectra were recorded at 0 °C at pH 4.00 in 1 M potassium fluoride, 1 mM potassium phosphate. Data were collected at 0.2 nm increments from 260 to 190 nm. Ellipticity at 222 nm was measured at pH* 4.00 or pH* 3.50 in ^2H_2O containing 1 M sodium chloride, 20 mM sodium phosphate. pH* is the glass electrode reading, uncorrected for isotope effects.

Ellipticity at 222 nm, θ_{222}, is assumed to be linearly related to mean helix content, f_H, which can be calculated from the Lifson−Roig-based helix−coil model (see below). The conversion of θ_{222} to f_H requires the knowledge of the base line ellipticities of both the random coil, θ_C, and the complete helix, θ_H:

$$f_H = (\theta_{222} - \theta_C)/(\theta_H - \theta_C) \quad (1)$$

The values of θ_C and θ_H are dependent on temperature and are given by the following expressions:

$$\theta_C = 2220 - 53T \quad (2a)$$

$$\theta_H = (-44\,000 + 250T)(1 - 3/N_r) \quad (2b)$$

where T is the temperature in °C and N_r is the chain length in residues. These expressions are those given by Luo and Baldwin (1997) and are determined by fitting the Lifson−Roig model for the helix−coil transition to the ellipticity of these peptides as a function of temperature and trifluoroethanol concentration.

NMR Spectroscopy. Samples were prepared by dissolving peptide in water to a concentration of 1−2 mM, adjusting to pH 3.5 or 4.0 (see below) with hydrochloric acid, and then lyophilizing to dryness. To initiate exchange, the peptide was dissolved at 1−2 mM in ^2H_2O containing 1 M sodium chloride, 20 mM sodium phosphate. After the peptide was dissolved in buffer, multiple one-dimensional proton spectra were acquired during the exchange on a General Electric GN-Omega spectrometer at a proton frequency of 500.13 MHz. Data were collected using a 5000 Hz spectral width and a 60° pulse. The FID was the sum of 64 scans collected in 4096 complex points with an acquisition time of 0.82 s and a 5 ms recycle delay. Spectra were processed using FELIX (Release 2.1, Biosym Inc.) on a Silicon Graphics Indigo computer. FIDs were multiplied by a exponential decay function with line broadening of 1 Hz prior to Fourier transformation. Proton occupancy was determined by measuring the integral of all peaks in the amide region of each spectrum. Under these experimental

conditions, the amide protons of the C-terminal blocking group and the ϵ-amino protons of the lysine side chains have high intrinsic exchange rates and are generally completely exchanged within the dead time of the experiment.

Exchange curves were measured at pH* 3.5, at 0.6, 11.1, 16.4, 21.6, and 26.9 °C and at pH* 4.0 at 5.9 °C. The temperature in the NMR probe was calibrated using the chemical shifts of methanol (Raiford et al., 1979). All reported pH* measurements were made after the acquisition of the NMR spectra. To facilitate comparison of the exchange behavior of these peptides, small differences in measured final pH* were corrected by expanding or contracting the time axis according to the equation

$$\text{time*} = (\text{time})[10^{(\text{experimental pH*})}]/[10^{(\text{corrected pH*})}] \quad (3)$$

where time* is the corrected time and the corrected pH* is either 4.00 (for exchange curves measured at 5.9 °C) or 3.50 (for all other exchange curves) . This correction is valid only for small interpolations in pH in the region where base-catalyzed exchange predominates (Rohl et al., 1992).

In the pH range of these experiments (pH* 3.5−4.0), exchange is base-catalyzed and occurs by the EX2 mechanism (Rohl et al., 1992; Rohl & Baldwin, 1994). Kinetic exchange curves for helical peptides were fitted as described previously (Rohl et al., 1992; Rohl & Baldwin, 1994) by assuming that a single amide proton cannot exchange when it is hydrogen bonded but freely exchanges when the helical hydrogen bond is broken. The observed exchange kinetics are the sum of the exchange curves of all individual protons, and the fractional proton occupancy as a function of time*, $f_o(t)$, is given by

$$f_o(t) = \sum_{i=1}^{N_r}(1/N_r)\exp[-(k_{int}[1 - f_B(i)])t] \quad (4)$$

where N_r is the chain length, k_{int} is the average exchange rate constant for a residue with a non-hydrogen-bonded amide proton, $f_B(i)$ is the probability that the amide proton of residue i is hydrogen-bonded, and t is time*. The peptides are treated as homopolymers in deriving the intrinsic exchange rate, k_{int}, and an average value is used for all residues. The probability that the NH of residue i is hydrogen bonded, $f_B(i)$, is determined by using the Lifson−Roig model (see below). All nonlinear least squares analysis was accomplished using the modified Gauss−Newton nonlinear function minimization program NONLIN (Johnson et al., 1981) on a Silicon Graphics Indigo computer. Confidence intervals are evaluated at 67%.

Application of Helix−Coil Theory. CD and NH exchange measurements are both interpreted using the Lifson−Roig (1961) model for the helix−coil transition modified to include N-capping. This model has been extensively described elsewhere (Rohl et al., 1996). In brief, residue conformations are defined by dihedral angles as either helical or nonhelical and statistical weights describing nucleation, υ, propagation, w, and N-capping, n, are assigned to residues on the basis of the conformation of the residue and its nearest neighbors. The partition function is calculated by summing over all possible peptide conformations and is a function of the chain length, N_r, and the helix parameters (w, υ, n) of each component residue. The peptides are treated here as homopolymers, and an average helix propagation propensity for alanine and lysine is computed. An N-cap propensity of 1.0 is assigned to lysine and alanine residues. All other helix parameters at 0 °C in water are set at the values reported by Rohl et al. (1996): $\langle\upsilon^2\rangle = 0.0013$, $w(\text{G}) = 0.048$, $n(\text{Ac}) = 5.9$. Sequence-specific interactions are assumed not to contribute to helix formation in these peptides. The N-cap propensities and the helix nucleation parameter are assumed to be temperature independent. Helix parameters in 40 vol % trifluoroethanol have been reported (Rohl et al., 1996), and for experiments in trifluoroethanol (see Discussion), the values of w(G) and n(Ac) were estimated by linearly interpolating between their values in water, and their values in 40 vol % trifluoroethanol [$w(\text{G}) = 0.098$, $n(\text{Ac}) = 4.0$].

Although Lifson−Roig-based models describe helix formation in terms of dihedral angles, the extent of hydrogen bond formation at a particular residue, $f_B(i)$, can be calculated from the helix−coil partition function [see also Rohl and Baldwin (1994)]. Three consecutive residues in the helical conformation are sufficient to align the peptide CO of residue $i-2$ and the peptide NH of residue $i+2$ to form a hydrogen bond. Because residues in the helical conformation with adjacent helical neighbors are defined as propagating residues in the Lifson−Roig model, each propagating residue is associated with an $i-2,i+2$ hydrogen bond. The probability that the peptide NH of residue i is hydrogen bonded, $f_B(i)$, is consequently equal to the probability that residue $i-2$ is a propagating helical residue assigned weight w. Mean helix content, f_H, is calculated by averaging the hydrogen bond probabilities of all residues which can hydrogen bond:

$$f_H = \langle n_H\rangle/(N_r - 2) \quad (5)$$

In this expression, $\langle n_H\rangle$ is the average number of helical hydrogen bonds formed and $N_r - 2$ is the number of hydrogen bonds possible in a peptide with N_r residues.

RESULTS

Temperature Dependence of Helix Content in Water. The peptides studied here have the sequence Ac-(AAKAA)$_n$GY-NH$_2$ and chain lengths of 7, 12, 17, and 22 residues. The design of sequences based on the repeat AAKAA has been discussed previously (Rohl et al., 1992). Such peptides show extensive helix formation because of the high helix propensity of alanine. In the peptide series examined here, the tyrosine included for concentration measurements is separated from the helix by a glycine residue to eliminate contributions to the CD bands arising from interactions of the tyrosine with the helix (Chakrabartty et al., 1993). The Lifson−Roig-based helix−coil model was fitted to the measured ellipticities of the 12-, 17-, and 22-residue peptides at varying temperatures using eqs 1 and 5 to obtain an average helix propensity, $\langle w\rangle$, at each temperature. The observed and best-fitted ellipiticities are in good agreement (Figure 1). The overall root-mean-square deviation between observed and predicted ellipticity is 600 deg cm^2 dmol^{-1}.

Total NH exchange curves for the four peptides in the series were measured in water at temperatures in the range 0.6−26.9 °C (Figure 2). The circular dichroism spectrum of the shortest peptide in the series, Ac-AAKAAGY-NH$_2$, indicates that it is unstructured at 0 °C (data not shown) and remains unstructured even upon addition of 50 vol % trifluoroethanol (Luo & Baldwin, 1997). A single exponential decay was fitted to the exchange curve of the 7-residue

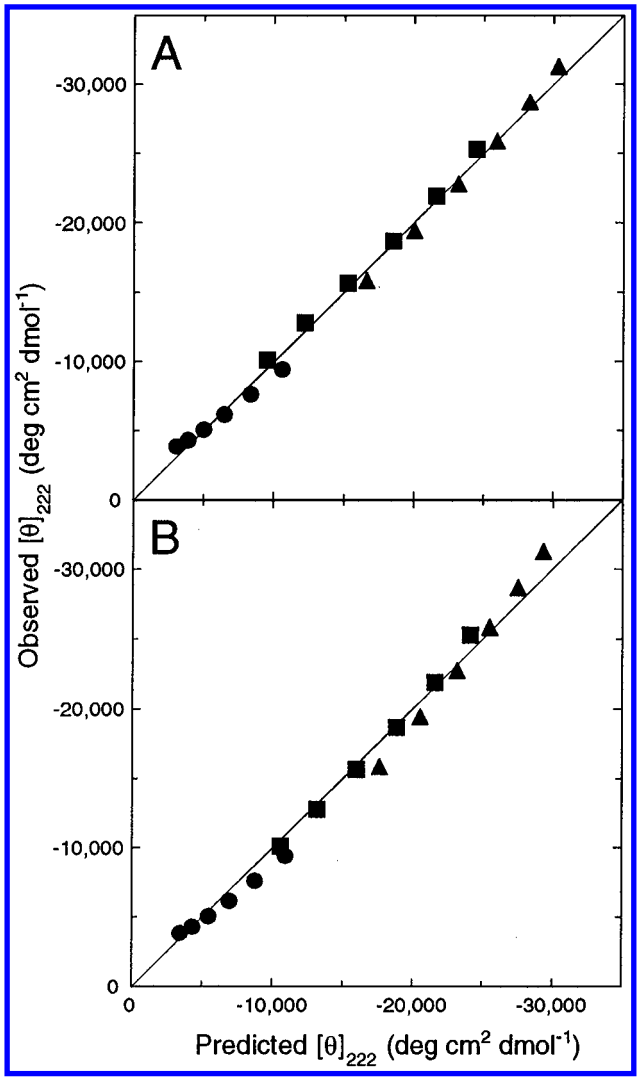

FIGURE 1: Correlation of predicted and observed ellipticities of Ac-(AAKAA)$_n$GY-NH$_2$ peptides. Measured ellipticities are reported for peptides with chain lengths of 12 (●), 17 (■), and 22 (▲) residues at 0.6, 5.9, 11.1, 16.4, 21.6, and 26.9 °C. All three peptides show decreasing ellipticity with increasing temperature. Predicted ellipticities are calculated from the modified Lifson−Roig helix−coil model using the best-fitted average helix propensity, $\langle w \rangle$, at each temperature (panel A) or using the values of $\langle w_0 \rangle$ and ΔH determined by NH exchange, and the fitted value of $\theta_H = -42100$ deg cm^2 dmol^{-1}. The root-mean-square deviations of the two correlations are 600 (panel A) and 945 deg cm^2 dmol^{-1} (panel B).

peptide at each temperature to obtain the observed average exchange rate constant, k_{obs}. k_{obs} shows Arrhenius behavior with a pre-exponential factor of 1.7×10^{13} min^{-1} and an activation energy of −19.0 kcal/mol (data not shown). The longer peptides in the series all show measurable helix formation in the temperature range from 0.6 to 26.9 °C, as indicated by their reduced rates of total NH exchange relative to the unstructured 7-residue peptide (see Figure 2). Equation 4 was fitted to the exchange curves of the helical peptides at each temperature by assuming that the intrinsic exchange rate constant, k_{int}, is equal to the observed exchange rate constant of the 7-residue peptide, k_{obs}, at each temperature.

The fitted values of the average helix propagation propensity, $\langle w \rangle$, at each temperature, determined by either CD or NH exchange, are shown in Figure 3. The temperature dependence of $\langle w \rangle$ can be described by the van't Hoff relationship:

$$\ln \langle w \rangle = \ln \langle w_0 \rangle - \Delta H_{vH}/R(1/T - 1/T_0) \qquad (6)$$

The reference temperature is chosen to be 0 °C ($T_0 = 273.15$ K). $\langle w_0 \rangle$ is the average helix propagation propensity at 0 °C and ΔH_{vH} is the van't Hoff enthalpy. This model fits the observed temperature dependence of the average helix propensity determined by CD with $\langle w_0 \rangle = 1.578 \pm 0.015$ and $\Delta H_{vH} = -1.28 \pm 0.08$ kcal mol^{-1} res^{-1}. Fitting eq 6 to the average helix propensities determined by NH exchange yields $\langle w_0 \rangle = 1.615 \pm 0.020$ and $\Delta H_{vH} = -1.23 \pm 0.12$ kcal mol^{-1} res^{-1}. The van't Hoff enthalpies determined by the two techniques are identical within error and are in good agreement with the value of approximately −1.3 kcal mol^{-1} res^{-1} estimated by Scholtz et al. (1991) from differential scanning calorimetry of a 50-residue, alanine-based helix.

Comparison of the Helix−Coil Parameters Measured by CD and NH Exchange. Although circular dichroism and NH exchange measurements yield identical values of the enthalpy of helix formation, the average helix propagation propensity determined by NH exchange is larger than that determined by CD at each temperature. What is the reason for the difference in helix parameters measured by the two techniques? The helix−coil model fits either the CD or the NH exchange data well, suggesting that the helix−coil transition theory is unlikely to be the source of this discrepancy. A more plausible explanation lies in the procedures which are employed to relate CD and NH exchange to helix formation. A simple linear model is used to convert ellipticity to mean helix content (eq 1). In the conversion of CD to mean f_H, the least well-determined parameter is the base line ellipticity of the complete helix as a function of temperature. The constants in eq 2b cannot be measured directly but must be determined by extrapolation using short peptide data (Luo & Baldwin, 1997). One possible explanation for the lower helix propensities measured by CD relative to NH exchange is that the value of −44000 deg cm^2 dmol^{-1} overestimates the ellipticity of the complete helix, and helix contents calculated from eq 1 are underpredicted. Although the value of 250 deg cm^2 dmol^{-1} °C^{-1}, describing the temperature dependence of the helical base line, is also somewhat ill-determined, error in this value can account for the observed discrepancies between helix contents monitored by the two techniques because lower propensities are measured by CD than by NH exchange at all temperatures.

NH exchange under EX2 conditions can be modeled simply as an equilibrium between closed and open states, which are incompetent and competent, respectively, for exchange, followed by a chemical exchange step (Hvidt, 1964). In the case of the peptide helix, the closed−open equilibrium is the formation of a single $i,i+4$ helical hydrogen bond. When the hydrogen bond is broken, the amide proton can exchange for a solvent deuteron with the rate constant, k_{int}:

$$(CO_{i-2}\cdots HN_{i+2}) \overset{K_{eq}(i)}{\longleftrightarrow} (CO_{i-2})(HN_{i+2}) \overset{k_{int}}{\longrightarrow} (CO_{i-2})(DN_{i+2}) \qquad (7)$$

The rate constant for the chemical exchange step, k_{int}, is not measured directly but is generally assumed to be equivalent

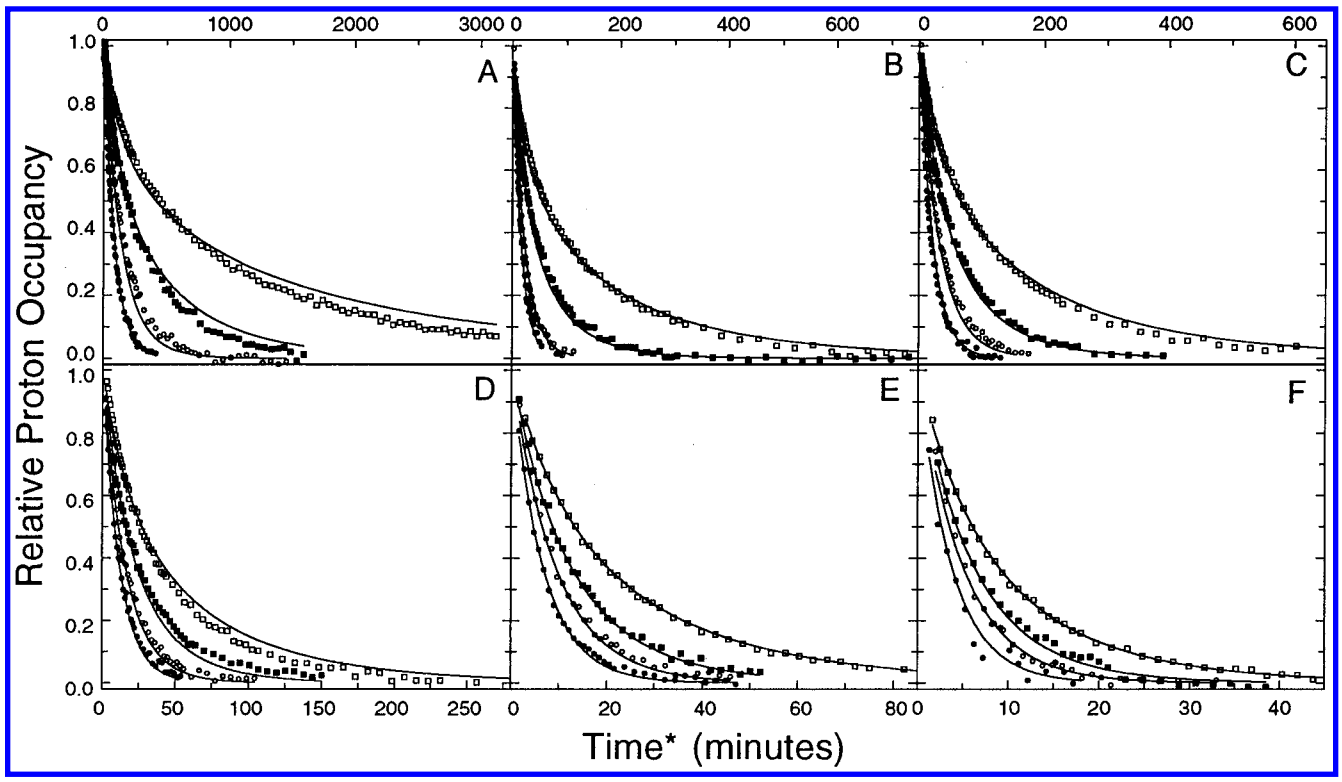

FIGURE 2: Exchange curves of Ac-(AAKAA)$_n$GY-NH$_2$ peptides in water. The relative proton occupancy of the amide region as a function of time is shown for peptides of chain length 7 (●), 12 (○), 17 (■) and 22 (□) residues at 0.6 (panel A), 5.9 (panel B), 11.1 (panel C), 16.4 (panel D), 21.6 (panel E), and 26.9 °C (panel F). Time* is calculated according to eq 3. The solid lines are fits to the data of either a single exponential (7-residue peptide) or eq 4 (12-, 17-, and 22-residue peptides) using the helix parameters determined from measured ellipticities and the best-fitted value of k_{int} (see text). Exchange curves calculated from eq 4 using the best-fitted helix parameters and k_{int} fixed at the value of rate constant measured for the 7-residue peptide yield nearly superimposable curves (see text).

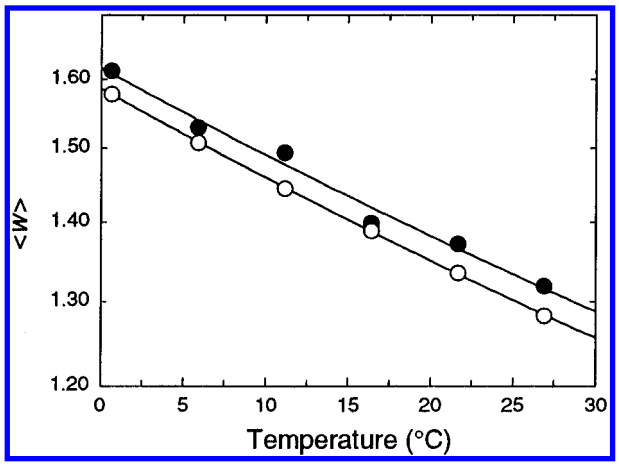

FIGURE 3: Temperature dependence of the measured helix propagation propensity in water. The best-fitted value of the average helix propagation propensity, $\langle w \rangle$, determined from either the measured ellipiticities (●) or the NH exchange curves (○) of the 12-, 17-, and 22-residue peptides, is shown on a log scale. The solid lines are the fits of the van't Hoff relation (eq 6) to the data.

to the exchange rate constant measured for model compounds. Here we have used the observed exchange rate constant, k_{obs}, measured for the unstructured 7-residue peptide, as the value of k_{int}. This assumption may not, however, be valid, because the environment from which exchange occurs in a helical peptide is likely to differ significantly from the bulk solvent (see Discussion). An alternative explanation for the larger helix propagation propensities measured by NH exchange is that the intrinsic exchange rate is slower in the helix than expected, based on the average exchange rate in the unstructured peptides.

To test the plausibility of these two possible explanations for the discrepancy between the helix contents measured by CD and NH exchange, we attempted to obtain a single set of helix parameters which predicts both data sets. When the helix−coil model is fitted to the measured ellipticities using eqs 1 and 5 and the helix parameters determined by NH exchange, the fitted value of θ_H decreases to −42100 deg cm^2 dmol^{-1}, and a significantly worse correlation between the predicted and measured ellipticities is found (Figure 1b). The root-mean-square deviation for the correlation increases from 600 to 945 deg cm^2 dmol^{-1}. When the converse procedure is followed and eq 4 is fitted to the NH exchange data using the helix parameters determined by circular dichroism, then the intrinsic exchange rate constant, k_{int}, is allowed to vary. The best-fitted curves, shown in Figure 2, are nearly superimposable with the best-fitted curves obtained by varying the helix parameters and setting the rate constant k_{int} equal to the value determined from the unstructured 7-residue peptide, k_{obs} (data not shown). At each temperature, the variance is actually slightly lower when $\langle w \rangle$ is held constant than when k_{int} is fixed. Both the NH exchange and the circular dichroism data can be fitted with the same set of helix parameters by removing the assumption that k_{int} is equal to k_{obs} for the unstructured 7-residue peptide.

The Intrinsic Exchange Rate Is Slower in a Partly Helical Peptide Than in the Random Coil. The correlation of the best-fitted values of k_{int} with the observed exchange rate constants for the 7-residue peptide (Figure 4) shows a slope of 0.83 ± 0.02, indicating that intrinsic exchange rate in the partly helical peptide is approximately 17% slower than the observed rate in the unstructured peptide. Although several

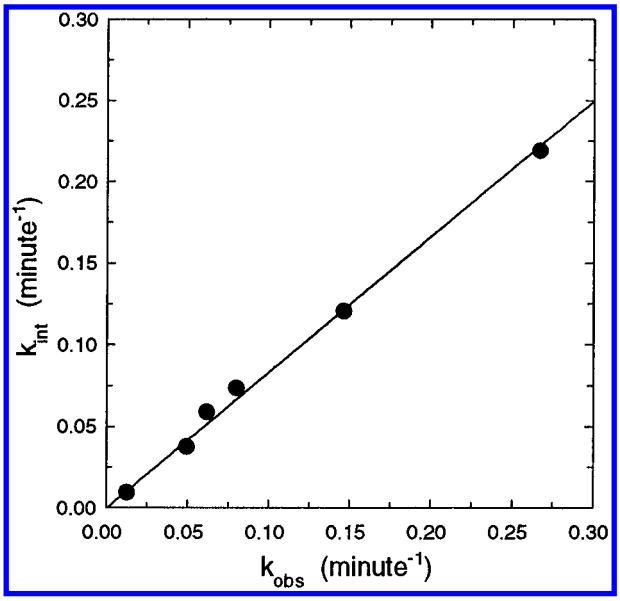

FIGURE 4: Correlation between the intrinsic exchange rate in a partly helical peptide and in the random coil. k_{obs} is the observed rate constant for exchange in the unstructured 7-residue peptide. k_{int} is the intrinsic exchange rate constant in the helical peptides, determined from fitting the exchange curves of the 12-, 17-, and 22-residue peptides to eq 4 using the helix parameters determined from measured ellipticities (see text).

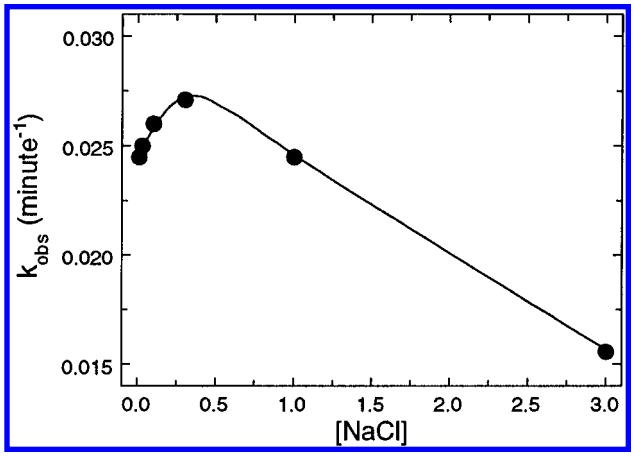

FIGURE 5: Effect of ionic strength on the exchange rate in the absence of structure. The observed exchange rate constant k_{obs} for total NH exchange from Ac-AAKAAGY-NH_2 is shown as a function of sodium chloride concentration at pH* 3.5, 5 °C. The solid line is drawn to guide the eye.

explanations may account for the difference between the intrinsic exchange rate in the partly helical peptides and the rate predicted from unstructured peptides, one possibility is that this difference is electrostatic in origin. The exchange reaction is base-catalyzed and sensitive to the electrostatic environment which may differ significantly between a partly helical, exchange-competent conformation, and a random coil. Although the exchange kinetics here have been measured in the presence of 1 M sodium chloride to screen electrostatic interactions, the exchange rate may be dependent on ionic strength even at high ionic strength. To test this possibility, the exchange rate of the unstructured peptide was measured as a function of sodium chloride concentration.

The base-catalyzed exchange rate measured for the unstructured 7-residue peptide shows a complicated dependence on ionic strength (Figure 5). The rate constant increases with increasing ionic strength at low sodium chloride concentration, while at high ionic strength, the rate constant decreases with increasing salt concentration. The observed behavior is strikingly similar to the measured dissociation of water as a function of sodium chloride concentration (Harned & Mannweiler, 1935), suggesting that ionic strength-dependent changes in the ionization constant of water dominate the measured effect of ionic strength on the base-catalyzed exchange rate in the absence of structure and are likely to obscure any electrostatic screening effects at high ionic strength.

DISCUSSION

Measurement of Helix Content by Circular Dichroism. The goal of this work is to compare directly CD and NH exchange as techniques for measuring helix formation as a test both of helix−coil transition theory and of the models employed to relate helix−coil transition theory to experimental data. Here we have used a linear relationship between ellipticity at 222 nm and the mean fraction helix content to extract the average helix propensity from measured ellipticities via the Lifson−Roig-based helix−coil transition model. The agreement between measured and fitted ellipticities is quite good, but some systematic deviations are observed: the measured ellipticity of the 12-residue peptide at each temperature is slightly lower than the fitted values, while the ellipticity of the 22-residue peptide is slightly higher than the fitted value, particularly when the helix content is largest. Systematic deviations of this sort are also observed for this length-dependent series in the complete thermal transitions of these peptides measured at varying trifluoroethanol concentrations, particularly at low temperatures where helix formation is maximal (Luo & Baldwin, 1997).

As pointed out by Shalongo and Stellwagen (1997), a linear relationship between ellipticity at 222 nm and fractional helix content is not strictly correct since the peptide molecules populate an ensemble of conformations containing helical segments of differing lengths and consequently, differing end effects. Shalongo and Stellwagen (1997) have recently proposed a statistical mechanical treatment of the dichroic contribution of the ensemble of partially helical states which results in a nonlinear relationship between mean helix content and mean molar ellipticity. Since peptides of different chain length will populate different ensembles of helical segment lengths, neglecting the statistical ensemble in converting mean helix content to ellipticity may result in a length-dependent error similar to that observed in Figure 1. In addition, Shalongo and Stellwagen note that since the dichroic chromophore is the peptide bond, peptide chain lengths should be counted in peptide units rather than residues for purposes of applying helix−coil transition theory to ellipiticity data. Since the difference in chain length counted by residue and peptide units becomes increasingly significant as chain length decreases, this correction is also expected to have a length-dependent effect.

To test the possibility that the length-dependent deviations observed in Figure 1 result from assumptions in the model relating helix−coil transition theory and measured ellipticities, we have implemented a statistical treatment of circular dichroism identical to the "dichroic statistical model" described by Shalongo and Stellwagen (1997), maintaining the base line ellipticities, temperature dependences, and chain

length correction as described in eqs 2a and 2b. When fitted to the measured ellipticities of the peptides studied here, the dichroic statistical model yields helix−coil transition parameters ($\langle w_0 \rangle = 1.575$ and $\Delta H_{vH} = -1.25$ kcal mol^{-1} res^{-1}) and calculated ellipticities that are identical within error to those determined by fitting eq 1 to the measured ellipticities. This result suggests that the linear relationship between ellipiticity and mean helix content, although a more approximate treatment than the statistical dichroic model proposed by Shalongo and Stellwagen, does not introduce significant error into the helix parameters or the ellipticities predicted by helix−coil transition theory for peptide helices in this range of length and helix content.

3_{10} Helix Formation. It has been proposed that alanine-based peptides show a significant population of 3_{10} helical turns, localized predominantly at the helix termini, under conditions where helix formation is marginal (Milhauser, 1995). The helix−coil transition model, which does not include 3_{10} helical turns, independently fits both NH exchange and CD data well, indicating that the model provides a reasonable description of the ensemble of conformations. Because 3_{10} helical turns are expected to be favored in short peptides and marginally stable helices, neglecting significant 3_{10} population should lead to systematic underprediction of the helix content of short peptides and peptides with low helix contents. Significant deviations between predicted and measured ellipticities are observed for the short 12-residue peptide, but these deviations are largest when the peptide helix is most stably formed, and the helix content of the short peptide is generally overpredicted, relative to the longer peptides, rather than underpredicted (Figure 1A). Similarly, in fitting the NH exchange curves, the most significant deviations between theory and experiment are found for the longest peptide at low temperature where the helix is most stable (Figure 2A), rather than for short peptides or peptides with low helix contents. In addition, since 3_{10} helical turns will contribute to both the measured ellipticity and the measured NH exchange kinetics, it is unlikely that 3_{10} helical turns can account for the observed quantitative discrepancy between helix parameters measured by CD and NH exchange. The difference in helix propensities measured by NH exchange and CD is fairly constant over the range of helix propensities examined and does not increase with decreasing propensity as would be expected if formation of 3_{10} helical turns significantly affect the interpretation of the data.

Reference Exchange Rates. A single set of helix parameters which predicts both CD and NH exchange data can be obtained by removing the assumption that the intrinsic exchange rate in the helix is equal to the exchange rate of the 7-residue reference peptide. A trivial explanation for the difference between the determined values of k_{int} and the observed exchange rate constants for the short peptide is that the 7-residue peptide is not an appropriate reference for the intrinsic exchange rate in the absence of structure. The reference peptide contains the same basic sequence repeat as the helical peptides, but is expected to be devoid of helical structure because of its short chain length. Although entropically unfavorable, the five-residue AAKAA block can theoretically form a single α-helical hydrogen bond, or two 3_{10} helical hydrogen bonds. No structure is detected, however, in this peptide by circular dichroism even upon addition of 50 vol % trifluoroethanol which greatly stabilizes the helical structure in all of the longer peptides (Luo & Baldwin, 1997). Additionally, if the 7-residue peptide had some minimal degree of structure, undetected by circular dichroism, the measured rate of exchange in this peptide would underestimate the true exchange rate of the random coil. Since the intrinsic exchange rate in the helix is found to be slower than the rate measured in the short peptide, this possibility cannot account for the observed discrepancy between the intrinsic exchange rate in the helix and the exchange rate of the 7-residue peptide.

Comparison of the measured exchange rate of the 7-residue peptide to the rate predicted from model compounds provides further support for the validity of the 7-residue peptide as an appropriate reference. The average exchange rate constant measured here for the 7-residue peptide is in good agreement with the values predicted from calibrations using model dipeptides (Bai et al., 1993). The observed exchange rate constant for the 7-residue peptide is generally 15−20% slower than the average rate constant predicted from data of Bai et al. using poly-D,L-alanine as the basis rate. This difference likely results at least in part from the lower ionic strength used by Bai et al. (0.5 M potassium chloride) relative to the conditions here (1.0 M sodium chloride), because the average exchange rate of the 7-residue peptide is expected to decrease between 0.5 and 1.0 M sodium chloride (see Figure 5). If the rate predicted from the data of Bai et al. is used as the reference for the intrinsic rate of exchange, then the slope in the correlation shown in Figure 4 decreases to 0.72, resulting in an even larger difference between k_{int} in the helix and the reference exchange rate.

Complex Exchange Kinetics in the Peptide Helix. The observed discrepancy between the intrinsic exchange rate in the peptide helix and the reference exchange rate measured either in the 7-residue peptide or predicted from model compound data suggests that intrinsic exchange in the helix is affected by interactions which do not contribute to exchange in model compounds. Such a result is not surprising since the exchange-competent conformation in a helical peptide is not completely disordered, and is likely differ from the random coil both electrostatically and sterically. The effect of electrostatics on the intrinsic exchange rate in the helix is likely to be complex. Rohl and Baldwin (1994) measured protection factors for base-catalyzed exchange for individual protons in an alanine-based helix. In general, the measured protection factors are larger than those predicted by the helix parameters determined from circular dichroism studies (Rohl & Baldwin, 1994), in agreement with the results discussed here. The deviation between predicted and measured protection factors is not, however, uniform. At the N-terminus of the helix, amide protons which cannot form hydrogen bonds exchange faster than predicted from unstructured peptides. These observations may again be consistent with an electrostatic effect on exchange rates: the difference between the intrinsic exchange rate and rates in model compounds may depend on the position within a helix, and/or the extent of helix formation.

The observed base-catalyzed exchange rate constant for the unstructured peptide changes nearly 2-fold over the salt concentration examined (Figure 5), and consequently the effect of changes in the ionization constant of water are likely to obscure any electrostatic screening effects remaining at high ionic strength. Although the origin of difference between the intrinsic exchange rate in the helix, and rates

measured in model compounds remains unclear, it appears that the exchange reaction in peptide helices becomes increasingly complex as the extent of helix formation increases, as suggested by the NH kinetics measured in 5, 10, and 15 vol % trifluoroethanol. The ellipticities of the Ac-$(AAKAA)_n$GY-NH_2 peptides measured in trifluoroethanol can be fitted using the modified Lifson−Roig model and the same nucleation parameter, v^2, at each trifluoroethanol concentration (Luo & Baldwin, 1997). This result suggests that the cooperativity of the transition does not change significantly upon addition of trifluoroethanol. The modified Lifson−Roig model cannot, however, be fitted to the NH exchange curves in trifluoroethanol using a nucleation parameter of 0.0013 (data not shown). When the CD-determined helix parameters are used to predict the NH exchange curves in trifluoroethanol, allowing the value of k_{int} to vary, the predicted curves deviate systematically from the observed curves: at early time points, the extent of exchange is over-predicted while at long time points, the extent of exchange is under-predicted. This behavior, which is observed to be small for the 22-residue peptide at 0 °C in the absence of trifluoroethanol (see Figure 2A), becomes appreciably worse with increasing trifluoroethanol concentration, suggesting that, as the helix content increases, more complicated exchange behavior is observed.

Implications for NH Exchange in Proteins. In native proteins or folding intermediates, intrinsic exchange rates cannot be measured directly, and protection factor measurements in these systems rely on exchange rates determined from model compounds (Molday et al., 1972; Bai et al., 1993) to predict the values of k_{int}. The largest protection factors measured in such studies should agree with the value calculated from the global stability of the protein. Often, however, larger global stabilities are measured by NH exchange than by optically monitored chemical denaturation [see for example Bai et al. (1994)]. The data here indicate that the problem probably arises from assuming that the actual exchange rate in the unfolded protein is the same as the exchange rate taken from model peptide data [see Mayo and Baldwin (1993) and Bai et al. (1994)]. Because charge effects are not included in the calibration based on model peptide data, there can be a serious discrepancy between the actual and assumed exchange rates in the unfolded protein. Exchange rates are known to depend on the local electrostatic potential (Kim & Baldwin, 1982), and salt effects on exchange have also been observed for neutral poly-D,L-alanine (Bai et al., 1993). Direct evidence that there can be significant electrostatic contributions to the exchange rate of amide protons in the denatured state of proteins is provided by exchange measurements in thermally denatured RNase A. Robertson and Baldwin (1991) observed shifts in the pH minima of exchange of as much as 0.45 pH units for amide protons in thermally denatured RNase A, relative to the minima predicted from model compound studies, and offered the high net positive charge of the polypeptide chain as a plausible explanation of this effect.

Although the alanine-based peptide helix is a relatively simple system, the intrinsic exchange rate in the helix deviates significantly from the rates predicted from model compounds. Direct comparison of NH exchange results and circular dichroism in helical peptides indicates that nearly 20% of the measured protection results solely from the change in the value of k_{int} rather than from hydrogen bond formation. Because such effects are likely to occur in proteins as well, these data suggest that apparent local free energies in proteins determined by NH exchange should be interpreted with caution.

ACKNOWLEDGMENT

We thank Dr. Stellwagen for providing a preprint of his manuscript. FAB mass spectra were provided by the Mass Spectrometry Facility, University of San Francisco, supported by a grant from the National Institutes of Health (RR 01614).

REFERENCES

Bai, Y., Milne, J. S., Mayne, L., & Englander, S. W. (1993) *Proteins: Struct. Funct. Genet. 17*, 75−86.
Bai, Y., Milne, J. S., Mayne, L., & Englander, S. W. (1994) *Proteins: Struct. Funct. Genet. 20*, 4−14.
Brandts, J. F., & Kaplan, L. J. (1973) *Biochemistry 12*, 2011−2024.
Chakarabartty, A., & Baldwin, R. L. (1995) *Adv. Protein Chem. 46*, 141−176.
Chakrabartty, A., Schellman, J. A., & Baldwin, R. L. (1991) *Nature 351*, 586−588.
Chakrabartty, A., Kortemme, T., Padmanabhan, S., & Baldwin, R. L. (1993) *Biochemistry 32*, 5560−5565.
Chakrabartty, A., Kortemme, T., & Baldwin, R. L. (1994) *Protein Sci. 3*, 843−852.
Doig, A. J., & Baldwin, R. L. (1995) *Protein Sci. 4*, 1325−1336.
Doig, A. J., Chakrabartty, A., Klingler, T. M., & Baldwin, R. L. (1994) *Biochemistry 33*, 3396−3403.
Englander, S. W., & Kallenbach, N. R. (1984) *Q. Rev. Biophys. 16*, 521−655.
Harned, H. S., & Mannweiler, G. E. (1935) *J. Am. Chem. Soc. 37*, 1873−1876.
Huyghues-Despointes, B. M. P., Klingler, T., & Baldwin, R. L. (1995) *Biochemistry 34*, 13267−13271.
Hvidt, A. (1964) *C.R. Trav. Lab. Carlsberg 34*, 299−317.
Johnson, M. L., Correia, J. J., Yphantis, D. A., & Halvorson, H. R. (1981) *Biophys. J. 36*, 575−588.
Kim, P. S, & Baldwin, R. L. (1982) *Biochemistry 21*, 1−5.
Lifson, S., & Roig, A. (1961) *J. Chem. Phys. 34*, 1963−1974.
Luo, P., & Baldwin, R. L. (1997) *Biochemistry 36*, 8413−8421.
Mayo, S. L., & Baldwin, R. L. (1993) *Science 262*, 873−876.
Millhauser, G. L. (1995) *Biochemistry 34*, 3873−3877.
Molday, R. W., Englander, S. W., & Kallen, R. G. (1972) *Biochemistry 11*, 150−158.
Raiford, D. S., Fisk, C. L., & Becker, E. D. (1979) *Anal. Chem. 51*, 2050−2051.
Robertson, A. D., & Baldwin, R. L. (1991) *Biochemistry 30*, 9907−9914.
Rohl, C. A., & Baldwin, R L. (1994) *Biochemistry 33*, 7760−7767.
Rohl, C. A., Scholtz, J. M., York, E. J., Stewart, J. M., & Baldwin, R. L. (1992) *Biochemistry 31*, 1263−1269.
Rohl, C. A., Chakrabartty, A., & Baldwin, R. L. (1996) *Protein Sci. 5*, 2623−2637.
Scholtz, J. M., Marqusee, S., Baldwin, R. L., York, E. J., Stewart, J. M., Santoro, M., & Bolen, D. W. (1991) *Proc. Natl. Acad. Sci. U.S.A. 88*, 2854−2858.
Shalongo, W., & Stellwagen, E. (1997) *Proteins: Struct. Funct. Genet.* (in press).
Stapley, B. J., Rohl, C. A., & Doig, A. J. (1995) *Protein Sci. 4*, 2383−2391.

BI9706677